Journal of Constructional Steel Research 205 (2023) 107811

Contents lists available at ScienceDirect

Journal of Constructional Steel Research

journal homepage: www.elsevier.com/locate/jcsr

Influence of uncertainties on the seismic performance of steel moment resisting frames

Melina Bosco, Elga Mangiameli, Pier Paolo Rossi *

Department of Civil Engineering and Architecture, University of Catania, Catania, Italy

ARTICLE INFO

Keywords:
Moment resisting frames
Seismic response
Uncertainties
Mean annual frequency of exceedance

ABSTRACT

The present paper investigates the probabilistic assessment of the seismic performance of steel MRFs designed according to Eurocodes. The considered MRFs are three- and five-storey high and are analysed by the multiple stripe method of analysis by means of sets of earthquake ground motions that depend in frequency content, energy and duration on the value of the selected seismic intensity measure. Additional uncertainties are related to the mechanical properties of steel, dead and live loads and equivalent viscous damping ratio. Different criteria are defined to assess the performance at the achievement of different limit states, in terms of interstorey drifts and damage indexes. To reach a synthetic evaluation of the seismic performances, the mean annual frequency of exceedance of the assigned limit state condition is also reported. Based on a Monte Carlo simulation the paper evaluates the effects of the single uncertainties on the seismic performances and suggests proper modifications to the simplified approach included in FEMA documents to mime the results of a full probabilistic approach.

1. Introduction

The probabilistic assessment of the seismic performance of buildings is gaining attention and popularity within the scientific community. In the framework of this approach, the assessment of the seismic performance is usually obtained by means of the estimate of the mean annual frequency of exceedance of a given set of limit state conditions generally involving either forces or displacements. The mean annual frequency of exceedance depends on the seismic hazard at the site and on the probability of exceedance of the assigned limit state conditions at different values of the selected ground motion intensity measure. The results of the assessment are significantly influenced by the simulation of the uncertainties of the main parameters involved in the structural and non-structural verifications [1–3]. As strongly influential for the results of the seismic assessment of constructions, seismic events should be simulated with care in order to represent the seismological characteristics of the expected earthquakes as well as the effects of the geotechnical and morphological conditions at the site. As a consequence, the earthquake ground motions should be selected (or artificially generated) to reflect the expected earthquake frequency content, energy and duration at the site. In addition, as underlined by many researchers, earthquake ground motions corresponding to different values of the seismic intensity measure should be selected to be representative of seismic events corresponding to the single assigned value of the selected intensity measure and should not be obtained by scaling of a single set of ground motions [4]. The magnitude of permanent and variable loads acting on constructions is sometimes also considered as an uncertain variable. In regard to permanent loads, Ellingwood et al. [5] proposed to describe the dead loads by means of a Gaussian probability distribution with a mean value equal to the characteristic value of the loads and a coefficient of variation equal to 0.10. This assumption is also in keeping with the current recommendations of Eurocode 0 [6]. Indeed, this code reports that, if the structure is sensitive to variations in the dead loads, the probability distribution of the magnitude of such loads should be assumed as Gaussian and the coefficient of variation should be in the range from 0.05 to 0.10 depending on the type of structure considered. Instead, to the best knowledge of the authors, the uncertainty in the magnitude and position of variable loads is generally neglected in literature.

Most research studies devoted to the probabilistic assessment of the seismic performance of structures also consider the variability of the material properties. In this regard, Baldassari et al. [7], collected data from three industrial producers and carried out statistical analyses to define mean, standard deviation, coefficient of variation, variance and 5% and 95% percentiles of the yield strength, tensile strength and elongation at maximum load of different structural profiles made of steel

* Corresponding author.
E-mail addresses: melina.bosco@unict.it (M. Bosco), elga.mangiameli@hotmail.it (E. Mangiameli), pierpaolo.rossi@unict.it (P.P. Rossi).

https://doi.org/10.1016/j.jcsr.2023.107811
Received 27 October 2022; Received in revised form 12 January 2023; Accepted 15 January 2023
Available online 14 March 2023

grade S235, S275, S355 or S460. Similarly, Simões da Silva et al. [8] collected data from several sources (e.g. [9–11]) and found that steel grade S235 exhibits the higher scatter of the mechanical properties (with a coefficient of variation equal to 0.10), maybe because steel profiles that cannot be classified as of higher steel grades are often classified as S235. Further, these researchers observed that, due to quality control procedures, the obtained minimum strength was always higher than the characteristic value. Based on the results of the tests reported in [12], Asgarian and Ordoubadi [2] proposed coefficients of variation equal to 0.11 and 0.065 for the yield and tensile strength of steel, respectively. Still in regard to the yield strength, the Italian code stipulates that, in qualification tests for steels members, a coefficient of variation equal to 0.08 should be used for steel grades from S235 to S355, whereas a coefficient of variation equal to 0.06 may be accepted for higher steel grades.

The uncertainty in the inherent damping is of some interest, particularly for the assessment of structures at the achievement of the serviceability limit states or, more in general, for the assessment of structures endowed with low dissipation energy capacities. In this regard, Porter et al. [13] summarized the experimental data on the variability of the equivalent viscous damping ratio obtained from 10 instrumented buildings (five steel-frame buildings, four buildings with reinforced-concrete frames, and one with reinforced concrete shear-walls) that experienced one or more than one ground motions [14]. Based on these results, a lognormal probability distribution with median equal to 0.05 and coefficient of variation equal to 0.4 was suggested for the equivalent viscous damping ratio [2,13,14].

The seismic performance is often obtained by means of Monte Carlo simulations and limit state functions that are expressed in terms of global (e.g. interstorey drift) or local response parameters (e.g. plastic rotation). However, in the case of large and complex structures numerous researchers also adopt simplifications in order to reduce the computational burden of the probabilistic analysis by means of the response surface methodology and/or by means of the first-order reliability method [15–18].

The application of the above probabilistic approach to some specific structural systems has led to a more refined and accurate assessment of the seismic performance of such systems. In addition, the comparison of these results with those from simpler numerical analyses in which uncertainties are not taken into account or are partially considered (for example, only in the frequency content of the ground motions) has underlined the difference between the results of the types of analysis. In this regard, aiming at miming the results a full probabilistic approach, FEMA documents [19,20] (devoted to the assessment of the seismic performance of buildings and to the evaluation of the seismic losses) state that accurate fragility curves can be obtained from analyses in which only uncertainties related to the seismic input (record to record uncertainty) are modelled, assuming that the other uncertainties do not modify the median response but only increase the dispersion β of the intensity measure of the fragility curve. The total dispersion (β_{tot}) is determined as the SRSS of the dispersions due to record-to-record variability (β_{RTR}) and other uncertainties (e.g. modelling-related uncertainty, test data-related uncertainty). The dispersion reported in these documents with reference to the single uncertainty does not depend on the structural type. In particular, to quantify the value of dispersion to be used, engineers have to formulate a quality judgment based on their experience on important issues such as the accuracy of the adopted numerical model.

In regard to steel moment resisting frames (MRFs), the probabilistic assessment of the seismic performance is carried out only in a few research studies. Two papers consider MRFs designed according to American codes [21,22] and uncertainties introduced in the cyclic behaviour of steel sections by means of probabilistically distributed parameters. Incremental dynamic analyses and Monte Carlo simulation are used to assess the seismic performance of refined models with specific beam-to-column joint elements. Out of keeping with FEMA documents, both the studies find that uncertainties mainly affect the median response of the considered buildings. However, due to the limited number of the structures (one MRF in [21] and two MRFs in [22]), the authors of the above papers state that further research is needed to reach general conclusions. More sources of uncertainty are considered in [2,23]. In particular, Vaez et al. [23] simulate the uncertainties in the modulus of steel, yield strength, gravity loads and thickness and width of parts of the cross-section. Based on the results of this research study, the authors state that the uncertainty in the modulus of elasticity, yield strength, section depth and geometry of the flange have the greatest effects on the maximum interstorey drift of the structure. The results, however, only refer to the response of two frames to seven ground motions characterised by a probability of exceedance of 10% in 50 years. Record-to-record uncertainties and other uncertainties related to the mechanical properties of steel, dead loads and equivalent viscous damping ratio are considered, instead, in a recent research study by Asgarian and Ordoubadi [2]. The influence of the uncertainties is investigated on two 5-storey 3-bay steel MRFs designed according to the Iranian Steel Design Code. The fragility curves are obtained through incremental dynamic analyses of centreline models without numerical modelling of beam-to-column joints. The earthquake ground motions (12 in number) are selected to simulate the expected seismicity on a soil category C based on NEHRP [24] and are scaled to represent the seismic input corresponding to different values of the seismic intensity measure. The researchers conclude that the uncertainties clearly affect the seismic performance of the steel MRFs and that the convenient assumption that the median-parameter model produces the median seismic performance is not necessarily true.

The present paper enters the line of research of the above authors to investigate with a high level of accuracy the probabilistic assessment of the seismic performance of steel MRFs designed according to Eurocodes. The considered MRFs are three- and five-storey high and are analysed by the multiple stripe method of analysis by means of sets of earthquake ground motions that depend in frequency content, energy and duration on the value of the selected seismic intensity measure. The model of the MRFs includes nonlinear elements that simulate the response of beams and columns and elements that simulate the response of the beam-to-column joint [25]. Additional uncertainties are related to the mechanical properties of steel, dead and live loads and equivalent viscous damping ratio. Different criteria are defined to assess the performance at the achievement of different limit states, in terms of forces, interstorey drifts and damage indexes. To reach a synthetic evaluation of the seismic performances, the mean annual frequency of exceedance of the assigned limit state condition is also reported. Based on a Monte Carlo simulation the paper evaluates the effects of the single uncertainties on the seismic performances and suggests proper modifications to the simplified approach included in FEMA documents [19,20] in order to mime the results of a full probabilistic approach.

2. Methodology

To investigate the effects of the uncertainties, the statistical distributions of the probabilistic variables have been preliminarily defined. Then, moment resisting frames are designed according to Eurocode 8 and the seismic response of each of the designed structures is determined considering 3 different approaches. In the first approach (analysis type #1), a model with median properties of the probabilistic variables is considered (model M) and the seismic response is evaluated by multiple stripe analysis (MSA) considering a set of 50 ground motions for each selected intensity measure. The results of the numerical analyses are elaborated by means of the maximum likelihood method [26,27] to obtain the fragility curves corresponding to the achievement of different limit states. The fragility curve is expressed as a function of two parameters, θ_M and β_{RTR}, that represent the median intensity measure corresponding to the achievement of the considered limit state and the record-to-record uncertainty, respectively. The parameters θ and β of the

fragility curves are determined maximizing the logarithm of the likelihood function, as reported in the following relation [26]

$$\{\hat{\theta}\ ,\ \hat{\beta}\} = \underset{\theta,\ \beta}{argmax} \sum_{j=1}^{m} \left\{ ln\left(\begin{matrix} n_j \\ z_j \end{matrix}\right) + z_j ln\Phi\left(\frac{ln(s_j/\theta)}{\beta}\right) + (n_j - z_j) ln\left[1 - \Phi\left(\frac{ln(s_j/\theta)}{\beta}\right)\right] \right\} \quad (1)$$

where n_j is the number of analyses that have been carried out at the intensity measure IM = s_j and z_j is the number of analyses in which the considered limit state has been exceeded. The obtained fragility curve is also used to evaluate the mean annual frequency of exceedance of the above-mentioned selected limit state.

In the second approach (analysis type #2), 50 numerical models (models U#01 to U#50) are generated by varying seismic mass, permanent and variable loads, equivalent viscous damping ratio and strength of steel according to assigned probabilistic distribution functions. Each numerical model is subjected to the action of a single accelerogram, which is extracted from the suite of the 50 ground motions artificially generated for the assigned earthquake return period. The obtained performances will be affected by the uncertainties related to the ground motion and to the uncertainties related to seismic mass, permanent and variable loads, equivalent viscous damping ratio and strength of steel. Therefore, a comparison between the results of Analysis type #1 and #2 will provide an estimate of the effects of the uncertainties of seismic mass, permanent and variable loads, equivalent viscous damping ratio and strength of steel.

In the third approach (analysis type #3), 50 numerical models are generated to investigate the effects of the uncertainty in the values of a single probabilistic variable, while the values of all the other variables are assumed to be fixed and equal to the median value. Specifically, in analysis #3–1 the uncertain variable is the strength of steel (models S#01 to S#50), in analysis #3–2 the uncertain variable is the equivalent viscous damping ratio (models D#01 to D#50) and in analysis #3–3 the uncertain variables are loads and masses (models L#01 to L#50). For each earthquake return period, one accelerogram is generated to match the median pseudo-acceleration and displacement response spectra considered in the previous approaches. The results of analyses type #3 are used to quantify the dispersion of the results due to uncertainties in the material strength (β_{mat}), equivalent viscous damping ratio (β_{ξ}) and loads (β_L).

Finally, to validate a simplified approach, such as the one given in FEMA documents, the fragility curve characterised by the median value θ provided by analysis type #1 and by a total dispersion (β_{tot}) determined as the SRSS of the single previously determined dispersions will be compared to that obtained by analysis type #2 where all the considered sources of uncertainty are simultaneously considered.

3. Design of the case studies

The present research study investigates the seismic response of two (in-plan and in-elevation) regular buildings. The plan is rectangular and equal at all storeys (the sides are 36 m long in the *x*-direction and 24 m in the *y*-direction) (Fig. 1). The first building is three storeys high while the second is five storeys high. The interstorey height is equal to 4 m at the first storey and 3.3 m at the other storeys. The structural scheme of the buildings consists of four frames in the *x*-direction and seven frames in the *y*-direction. The spans are equal to 6 m in the *x*- direction and 8 m in the *y*-direction.

The frames in the *x*-direction are moment resisting and endowed with rigid connections. The frames in the *y*-direction are concentrically braced and endowed with pinned connections. All the columns are oriented with their strong axis parallel to the *x*-direction.

The buildings are founded on rock soil (category A soil in Eurocode 8) and are located in a moderate seismic zone. The expected peak

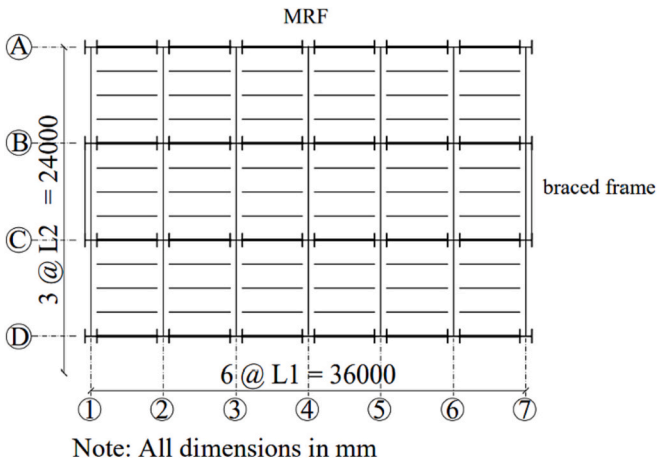

Fig. 1. Layout of the considered buildings.

ground acceleration with a probability of exceedance of 10% in 50 years is equal to 0.2779 g. For the same probability of exceedance, the upper period of vibration of the constant spectral acceleration branch of the spectrum (T_C) is equal to 0.43 s; in the same branch, the ratio F_O of the spectral acceleration to the peak ground acceleration is equal to 2.28.

The buildings are category of use type C according to the Italian code NTC18. The characteristic values of the permanent and variable loads on the floors are $g_k = 5.2$ kN/m^2 and $q_k = 3$ kN/m^2.

The external infill extends over the entire perimeter of the buildings and is characterised by a load per meter equal to $G_k = 4$ kN/m.

The buildings are designed to be highly ductile in keeping with the current version of Eurocode 8 [28]. According to this code, the reference value of the behaviour factor q of steel structures that are regular in elevation depends on the class of ductility (medium ductility class DCM or high ductility class DCH). The reference value of the behaviour factor is equal to 4 for frames in medium ductility class and 5.0 α_u/α_1 for frames in high ductility class. In the absence of more in-depth analyses, the α_u/α_1 ratio of multi-span multi-storey frames can be assumed equal to 1.3, leading to a maximum value of the behaviour factor equal to 6.5.

As prescribed in Eurocode 8 (EC8), second order effects are considered by means of the interstorey drift sensitivity coefficient through the following relation:

$$\theta = \frac{P_{tot}\ d_r}{V_{tot}\ h} \quad (2)$$

where P_{tot} is the total gravity load at and above the floor considered in the seismic design condition, V_{tot} is the total seismic storey shear force, h is the interstorey height and d_r is the inelastic interstorey drift, evaluated as the difference between the average lateral displacements at the top and at the base of the storey under examination. If the maximum value of θ is < 0.1, no amplification of the seismic action due to the second order effects is required; if $0.1 < \theta \leq 0.2$ the second order effects can be approximately taken into account by multiplying the first order seismic action effects by means of a factor equal to $1/(1 - \theta)$; if $0.2 < \theta \leq 0.3$ second order effects should be taken into account directly by using an established method of second-order analysis which takes account of geometric non-linearity; values of θ higher than 0.3 are not accepted.

For the verification of the interstorey drifts at the limited damage limit state, the interstorey displacements d_r are determined by a modal response spectrum analysis considering the pseudo acceleration response spectrum corresponding to earthquake return periods equal to 50 years in the considered seismic zone. For this return period, the peak ground acceleration, the period T_C and the amplification factor F_O are equal to 0.0687 g, 0.27 s and 2.519, respectively. The limit value of the interstorey drift is assumed equal to 0.005 times the interstorey height, as suggested in EC8 for buildings with fragile non-structural elements

attached to the structure. If the interstorey drift demand exceeds this limit, the behaviour factor used in design is reduced.

Lateral and lateral-torsional buckling of beams are assumed to be prevented by the slab of the deck. According to EC8, the plastic bending moment and the rotation capacity of the beams are verified to be not reduced by the axial and shear forces. In particular, referring to sections belonging to Classes 1 and 2, the following relationships are verified where the formation of the hinges is expected:

$$\frac{M_{Ed}}{M_{pl,Rd}} \leq 1.0 \tag{3}$$

$$\frac{N_{Ed}}{N_{pl,Rd}} \leq 0.15 \tag{4}$$

$$\frac{V_{Ed}}{V_{pl,Rd}} \leq 0.5 \tag{5}$$

where M_{Ed} is the design value of the bending moment, N_{Ed} is the design value of the axial force, V_{Ed} is the design value of the shear force, $M_{pl,Rd}$ is the plastic resistance to bending moments, $N_{pl,Rd}$ is the plastic resistance to axial forces and $V_{pl,Rd}$ is the plastic resistance to shear forces. The shear force V_{Ed} is equal to $V_{Ed,G} + V_{Ed,M}$ where $V_{Ed,G}$ is the design shear force due to the gravity loads in the seismic design situation and $V_{Ed,M}$ is the shear force due to the plastic bending moments in the ending cross-sections of the beam.

Columns are checked for instability considering the most unfavorable combination of the axial force and bending moment. The design internal forces are calculated by means of the following relations:

$$N_{Ed} = N_{Ed,G} + 1.1\ \gamma_{ov}\ \Omega\ N_{Ed,E} \tag{6}$$

$$M_{Ed} = M_{Ed,G} + 1.1\ \gamma_{ov}\ \Omega\ M_{Ed,E} \tag{7}$$

$$V_{Ed} = V_{Ed,G} + 1.1\ \gamma_{ov}\ \Omega\ V_{Ed,E} \tag{8}$$

where $N_{Ed,G}$, $M_{Ed,G}$ and $V_{Ed,G}$ are the axial force, the bending moment and the shear force in the column because of non-seismic actions; $N_{Ed,E}$, $M_{Ed,E}$ and $V_{Ed,E}$ are the axial force, bending moment and shear force in the column caused by seismic actions in the first order analysis carried out in design; γ_{ov} is the material overstrength factor and Ω is the minimum value of $\Omega_i = (M_{pl,Rd,i} - M_{Ed,G,i})/M_{Ed,E,i}$ of all the beams in which dissipative zones are expected.

Further, to promote a collapse mechanism in which dissipative zones are located at the ends of beams, the sum of the design values of the plastic resistances of the columns (reduced because of the axial force) framing into the joint has been verified to be larger than 1.3 times the sum of the plastic resistances of the beams framing into the same joint.

The shear strength of the core of the nodal panel has to satisfy the following expression:

$$\frac{V_{wp,Ed}}{V_{wp,Rd}} \leq 1.0 \tag{9}$$

where $V_{wp,Ed}$ is the design shear force in the panel due to the seismic action effects, taking into account the plastic resistance of adjacent dissipative zones in the beams or connections; $V_{wp,Rd}$ is the design shear resistance of the panel. The shear force in the panel is here calculated according to the principles of the capacity design and neglecting any beneficial effect provided by the shear force at the bottom of the upper column, by means of the following expression:

$$V_{wp,Ed} = \frac{M_{sx}}{h_t - t_f} + \frac{M_{dx}}{h_t - t_f} \tag{10}$$

where h_t is the depth of the beam, t_f is the thickness of the beam flange, M_{sx} and M_{dx} are the bending moments at the left and right sides of the joint (in the case of a side column, only one term shall be considered) and are determined taking into account the plastic resistance of the adjacent dissipative zones in beams or connections. In particular, the bending moments M_{sx} and M_{dx} are calculated by means of the relation:

$$M_{sx}(M_{dx}) = \sum \left[1.1\ \gamma_{ov}\left(M_{pl,Rd} + s_h\ V_{Ed,M}\right) + s_h\ V_{Ed,G}\right] \tag{11}$$

where s_h is the distance between the center of the plastic hinge and the axis of the column.

The shear strength of the panel $V_{wp,Rd}$ is calculated by means of the following relation:

$$V_{wp,Rd} = V_{wp,Rd,c} + V_{st,Rd} \tag{12}$$

where $V_{wp,Rd,c}$ is the shear strength of the web of the column and $V_{st,Rd}$ is the shear strength of the stiffeners.

The shear strength of the web $V_{wp,Rd,c}$ is calculated according to Eurocode 3 Part 1–8:

$$V_{wp,Rd,c} = \frac{0.9\ A_v\ f_{yk}}{\sqrt{3}\ \gamma_{M0}} \tag{13}$$

where A_v is the shear area of the column, f_{yk} is the characteristic value of the yield strength of steel of the column and γ_{M0} is a partial safety coefficient equal to 1.05.

The shear strength of the stiffeners $V_{st,Rd}$ is given by the relation:

$$V_{st,Rd} = \frac{0.9\ h_c\ t_p\ f_{yk}}{\sqrt{3}\ \gamma_{M0}} \tag{14}$$

where h_c is the depth of the column and t_p is the thickness of the stiffener.

4. Statistical characterization of the uncertainties

4.1. Ground motions and seismic hazard

The seismic hazard of the site under consideration has been defined based on the studies carried out by the INGV and the Department of Civil Protection of Italy [29,30]. These studies led to the definition of the probabilistic seismic hazard at the points of a regular grid (step equal to 0.05° in latitude and longitude) over the entire Italian territory. For each of these points, elastic response spectra varying in shape were provided for three percentiles of the pseudo-accelerations $S_{a,16\%}^{T_R}$, $S_{a,50\%}^{T_R}$ and $S_{a,84\%}^{T_R}$ (respectively equal to 16%, 50% and 84%) and for nine probabilities of exceedance P_{VR} (81, 63, 50, 39, 30, 22, 10, 5 and 2%) in a reference period of time of 50 years. Specifically, pseudo-accelerations were given for eleven periods of vibration T_i (equal to 0.0, 0.10, 0.15, 0.20, 0.30, 0.40, 0.50, 0.75, 1.00, 1.50, and 2.00 s). For the site under investigation, suites of artificially generated ground motions have recently been generated [31], which are compatible with the seismic hazard of the above site in terms of (i) median pseudo-acceleration, standard deviation of the pseudo-accelerations at given periods of vibration and (ii) correlation coefficients between pseudo-accelerations at different periods of vibration.

As an example, Fig. 2a shows the pseudo-acceleration spectra of the single ground motions, the target 16%, 50% and 84% spectra corresponding to a probability of exceedance equal to 10% in 50 years and the obtained 16%, 50% and 84% spectra.

To estimate the fragility curves accurately, pseudo-acceleration spectra corresponding to probabilities of exceedance P_{VR} not considered by INGV (i.e. 19, 16, 7, 1.5, 1.0, 0.75% in a reference period of time of 50 years) have been derived for the present research study. To this end, the return periods T_R corresponding to the eleven probabilities of exceedance in 50 years considered by INGV [29,30] have been first calculated as

$$T_R = -\frac{50}{ln(1 - P_{VR})} \tag{15}$$

Then, as suggested in CNR-DT 212/2013 [32], the seismic hazard

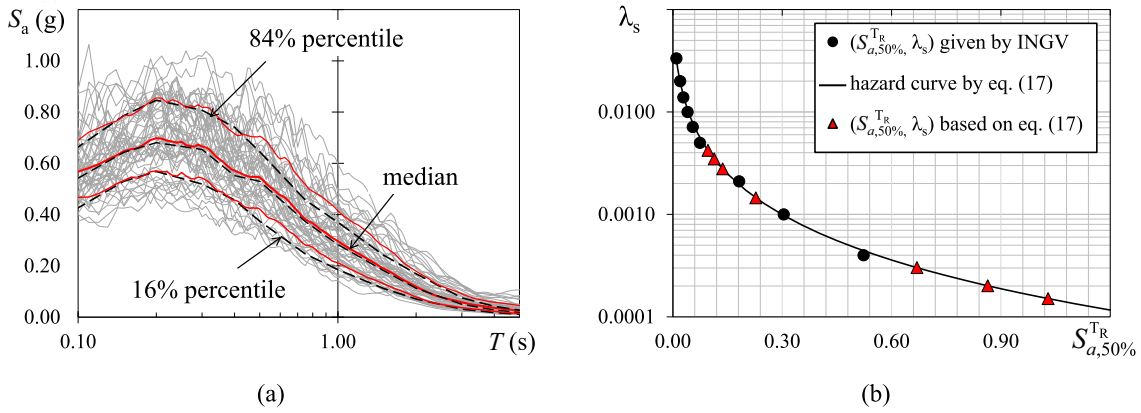

Fig. 2. Seismic hazard at the site: (a) response spectra for $P_{VR} = 10\%$ in 50 years; (b) hazard curve for $T_i = 1.50$s.

corresponding to T_R has been calculated as

$$\lambda_S = 1/T_R \tag{16}$$

Finally, for each of the eleven periods of vibration T_i, the pseudo-accelerations $S^{T_R}_{a,16\%}$,$S^{T_R}_{a,50\%}$ and $S^{T_R}_{a,84\%}$ have been plotted in a pseudo-acceleration versus seismic hazard coordinate system and a quadratic function has been calibrated in a logarithmic space to match the relation between the seismic hazard and the pseudo-acceleration. The quadratic function is expressed by means of the following relation:

$$\lambda_S(S_a) = k_0 \ \ exp\left(-k_1 ln\, S_a - k_2 ln^2 S_a\right) \tag{17}$$

where k_0, k_1 and k_2 are the parameters to calibrate.

The pseudo-accelerations $S^{T_R}_{a,16\%}$, $S^{T_R}_{a,50\%}$ and $S^{T_R}_{a,84\%}$ corresponding to the additional probabilities of exceedance P_{VR} are determined so as to provide the seismic hazard predicted by Eq. (4). As an example, Fig. 2b shows the pseudo-accelerations $S^{T_R}_{a,50\%}$ provided by INGV (black dots), the additional pseudo-accelerations $S^{T_R}_{a,50\%}$ (red triangles) and the calibrated quadratic function (continuous line) for a period of vibration equal to 1.50 s.

Once the target spectra have been determined, the procedure described in [31] has been used to generate a suite of 50 accelerograms for each considered probability of exceedance. The above-mentioned suites of accelerograms have been used as the seismic input for analyses type #1 and #2. For each seismic intensity level, the median pseudo-acceleration and displacement response spectra of the accelerograms have been calculated and assumed as the target to generate by the SIMQKE computer program [33] the additional single accelerograms that will be used in analysis type #3 where the uncertainties of seismic mass, permanent and variable loads, equivalent viscous damping ratio and strength of steel are separately considered.

4.2. Equivalent viscous damping ratio

The lognormal distribution is selected to describe probabilistically the equivalent viscous damping ratio. Starting from the research studies by Porter [13] and McVerry [14] and considering only the equivalent viscous damping ratios recorded in steel buildings under low intensity peak ground accelerations (as reported in Table 1), a mean value of 4.42%, a median value of 4.15% and a standard deviation of 1.706% have resulted.

4.3. Permanent and variable loads

Permanent and variable loads are described by a Gaussian probabilistic function. The coefficient of variation of the permanent loads is assumed equal to 0.1 [5]. The values of the mean and standard deviation of the variable loads, instead, are derived based on the definition of the

Table 1
Summary of identification studies used to estimate the uncertainty in the equivalent viscous damping ratio.

Building	Earthquake	Direction	Damping
JPL Building 180 Pasadena	Borrego Mountain	longitudinal	2.9%
		transverse	2.7%
	Lytle Creek	longitudinal	4.7%
		transverse	3.5%
Union Bank Building 445 South Figueroa Street	San Fernando	longitudinal	3.8%
		transverse	6.4%
	San Fernando	longitudinal	4.4%
		transverse	4.1%
KB Valley Center, 15,910 Ventura Boulevard	San Fernando	longitudinal	6.3%
		transverse	8.6%
Kajima International, 250 E. First	San Fernando	N36E component	3.8%
		N54W component	3.6%

frequent ($\psi_1 Q_k$) and quasi-permanent values ($\psi_2 Q_k$) of the variable loads, as provided in Eurocode 0 and in the Italian code [34]. Indeed, the quasi-permanent value is defined as the average value of load over a reference period of time, whereas the frequent value is defined as the 95% percentile of the temporal distribution of the load intensity. Based on these definitions, the mean value of the variable load is set equal to $\psi_2 Q_k$ whereas the standard deviation is equal to:

$$\sigma = (\psi_1 - \psi_2)\, Q_k / 1.645 \tag{18}$$

For the considered occupation type, the values of Q_k, ψ_1 and ψ_2 given by the Italian seismic code are 3.0 kN/m^2, 0.7 and 0.6. This leads to a standard deviation equal to 0.1824 kN/m^2.

The values of the permanent and variable loads are randomly generated to simulate the above-mentioned Gaussian distribution functions. In particular, one value of permanent load, one value of external infill load per meter and one value of variable load are generated for each single storey. The mass is calculated based on the generated values of the permanent and variable loads. Owing to this, some in-elevation irregularity can be generated by the assigned distribution of mass, whereas the in-plan irregularity (caused by asymmetric distribution of the mass within a single storey) is neglected.

4.4. Mechanical properties of steel

The values of the yield strength f_y are randomly generated to simulate a Gaussian distribution of values and assigned to the single members. In keeping with the Italian Code [34], the coefficient of variation COV of the yield strength is fixed equal to 0.06 in the case of characteristic yield strengths larger than 355 MPa and equal to 0.08 in all the

other cases. In the steel model that will be used in the numerical analysis (Menegotto-Pinto material model), the elastic and hardening moduli of steel E_s are assumed constant.

5. Numerical models

The MRF system is modelled in Opensees [35] as a two-dimensional centreline model. Columns and beams are schematised by means of elements endowed with concentrated plasticity over specified hinge lengths at the element ends. The length of the hinge is equal to the depth of the cross-section. Cross-sections are discretized into fibres: specifically, ten layers are considered across the thickness of the flanges and five across the depth of the web. The response of steel is simulated by means of the Menegotto-Pinto uniaxial material model. The elastic modulus is equal to 210,000 MPa, the strain-hardening ratio is equal to 0.3%, coefficient R_0 is equal to 20 and c_{R1} and c_{R2} are equal to 0.925 and 0.15, respectively. No isotropic strain hardening is considered.

The ends of the beams are constrained to develop equal horizontal displacements. However, to avoid significant axial forces in beams, three uniaxial springs are inserted at the ends of these members. The translational spring in the direction orthogonal to the longitudinal axis of the member and the rotational spring are characterised by high stiffnesses, so as to ensure virtually equal shear deformations and flexural curvatures on either side of the spring. The translational springs in the direction parallel to the longitudinal axis are characterised instead by low stiffness to avoid the development of high axial forces [36]. The beam-to-column joint is modelled as suggested in [37–25]. Details are provided in Subsection 5.1.

To consider P-Δ effects, a dummy column has been added to the model. This column is subjected at each storey to the entire gravity load of the storey and does not alter the lateral stiffness of the system because consisting of a series of elastic rigid truss members.

5.1. The panel zone

The panel zone is modelled as an articulated quadrilateral, as suggested by Gupta and Krawinkler [37]. The response of the panel zone is modelled by means of a trilinear rotational spring in one of the four corners; the remaining three corners are pinned. The centroid of the rigid elements of the panel zone model coincides with the intersection of beam and column longitudinal axes. The nonlinear behaviour of the rotational spring is formulated according to the recent proposal by Skiadopoulos et al. [25] as a function of the shear force - shear distortion angle response of the panel zone.

The elastic stiffness K_e of the panel zone, i.e. the ratio of the shear force to the shear distortion angle, is given by the following relation:

$$K_e = \frac{K_s K_b}{K_s + K_b} \tag{19}$$

where K_s is the stiffness contribution due to the shear deformation mode and K_b is the contribution due to the bending deformation mode. These latter terms are calculated by means of the relations:

$$K_s = t_{pz}\left(d_c - t_{cf}\right)G \tag{20}$$

$$K_b = \frac{12EI}{d_b^3}d_b \tag{21}$$

where t_{pz} is the thickness of the panel zone, t_{cf} is the thickness of the column flange, d_b is the depth of the beam cross-section and I is the moment of inertia of the column cross-section (including the doubler plate thickness, if any).

The yield strength V_y and the post-yield strength V_p of the panel zone were calculated by Skiadopoulos et al. [25] starting from distributions of tangential stresses resulting from finite element analyses of numerical models in which different geometries of the panel zone and beam and column cross-sections were considered. In particular, the shear strengths were calculated at three levels of shear distortion equal to γ_y, $4\gamma_y$ and $6\gamma_y$. Based on regression of the numerical results, Skiadopoulos et al. [25] recommended to calculate the yield strength of the panel zone by means of the relation

$$V_y = \frac{f_y}{\sqrt{3}}a_y\left(d_c - t_{cf}\right)\ t_{pz} \tag{22}$$

The shear strength of the panel zone corresponding to $4\gamma_y$ and $6\gamma_y$ was expressed by means of the following relation

$$V_{pz} = \frac{f_y}{\sqrt{3}}\left[a_{w,eff}\left(d_c - t_{cf}\right)\ t_{pz} + a_{f,eff}\left(b_{cf} - t_{pz}\right)\ 2t_{cf}\right] \tag{23}$$

where b_{cf} is the width of the column flange, $a_{w,eff}$ is the average shear stress within the column web and $a_{f,eff}$ is the average shear stress within the column flanges. The recommended values of a_y, and of coefficients $a_{w,eff}$ and $a_{f,eff}$ for distortions equal to $4\gamma_y$ and $6\gamma_y$ are reported in Fig. 3.

Coefficients a_y and $a_{f,eff}$ were suggested as a function of the ratio of the stiffness of the column flange K_f to the elastic stiffness of the panel zone K_e. To this end, the stiffness K_f was calculated by means of the relation

$$K_f = \frac{K_{sf}K_{bf}}{K_{sf} + K_{bf}} \tag{24}$$

In the above equation, the stiffness contributions due to shear deformation mode (K_{sf}) and bending deformation mode (K_{bf}) are given by the following relations:

$$K_{sf} = 2\left(t_{cf}b_{cf}G\right) \tag{25}$$

$$K_{bf} = 2\left[\frac{12E\left(b_{cf}t_{cf}^3/12\right)}{d_b^3}d_b\right] \tag{26}$$

The values of the bending moments corresponding to V_y and V_{pz} to be assigned to the rotational spring are evaluated by multiplying the relevant values of shear by the depth of the beam cross-section.

Null damping coefficient is assigned to the rigid elements of the panel zone model.

6. Numerical analyses and response parameters

The seismic response of the structures is determined by multiple stripe analysis. In the single nonlinear dynamic analysis, the damping matrix is defined as a linear combination of the mass and committed stiffness matrix. The proportionality coefficients for mass and stiffness matrices are defined so as to have the prefixed value of the equivalent viscous damping ratio for the first and second modes of vibration of the system.

At each instant of the nonlinear dynamic analysis, the response is determined in terms of global and local response parameters. The global parameters are the transient interstorey drifts and the residual interstorey drifts. The local response parameters are the damage indexes DI at the ends of beams and columns, the damage index of the panel zone (PI) and the lateral stability (SI) and lateral torsional stability (TI) indexes of columns.

The DI of beams and columns are calculated as the ratio of the plastic rotation demand (θ_{pl}) to the plastic rotation capacity (θ_u). In particular, the plastic rotation demand is calculated as

$$\theta_{pl}(t) = \left[\chi(t) - \frac{M(t)}{EI}\right]L_{pl} \tag{27}$$

where χ and M are the curvature and the bending moment recorded at the integration points located at the ends of the member, L_{pl} is the length of the plastic hinge, I is the moment of inertia of the member cross-sections and E is the elastic modulus of steel.

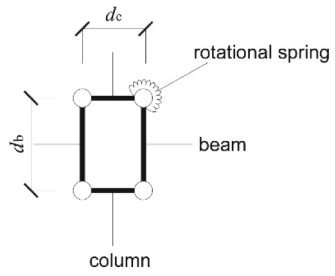

(a)

Parameter	Recommended value
a_y	$(0.58K_f/K_e+0.88)/(1-K_f/K_e)$
$a_{w,eff}$ $(4\gamma_y)$	1.10
$a_{w,eff}$ $(6\gamma_y)$	1.15
$a_{f,eff}$ $(4\gamma_y)$	$0.93K_f/K_e+0.015$
$a_{f,eff}$ $(6\gamma_y)$	$1.05K_f/K_e+0.020$

(b)

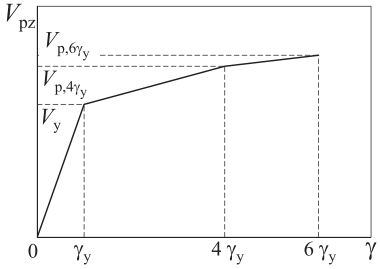

(c)

Fig. 3. Panel zone: (a) numerical model; (b) values of the response parameters for the evaluation of the shear resistance; (c) shear force versus shear distortion behaviour.

The plastic rotation capacity θ_u is expressed as a multiple of the chord rotation at yield, θ_y. Specifically, for beams and columns with dimensionless axial load $\nu \leq 0.30$, the plastic rotation capacity θ_u is equal to 8 θ_y if sections are Class 1 and 3 θ_y is sections are Class 2. A fragile behaviour is assumed for columns with $\nu > 0.50$. Linear interpolation is used to estimate the plastic rotation capacity of columns if ν is in the range from 0.3 to 0.5.

The chord rotation at yield is calculated as

$$\theta_y = \frac{M_{N,Rd} L_b}{6EI} \tag{28}$$

where L_b is the length of the member and $M_{N,Rd}$ is the plastic flexural resistance reduced because of the interaction with the axial force N_{Ed} (if present).

The damage index of the panel zone (PI) is calculated as the maximum of the ratios of the shear distortion γ (t) recorded during the time-history analysis to the shear distortion at ultimate. According to the draft of the revised version of Eurocode 8 [38], the shear distortion at ultimate is set equal to 4 γ_y.

Stability indexes are calculated for columns from the provisions given in Eurocode 3 [39]. In particular, the lateral stability (SI) index is given as

$$SI = max\begin{cases} \dfrac{N_{Ed}(t)}{N_{b,Rd,y}} + k_{yy}\dfrac{M_{Ed,y}(t)}{M_{pl,Rd,y}} + k_{yz}\dfrac{M_{Ed,z}(t)}{M_{pl,Rd,z}} \\ \dfrac{N_{Ed}(t)}{N_{b,Rd,z}} + k_{zy}\dfrac{M_{Ed,y}(t)}{M_{pl,Rd,y}} + k_{zz}\dfrac{M_{Ed,z}(t)}{M_{pl,Rd,z}} \end{cases} \tag{29}$$

where M_{Ed}(t) and N_{Ed}(t) are the bending moment and the axial force at the generic instant t of the time history, $N_{b.Rd,y}$ and $N_{b,Rd,z}$ are the buckling resistances with respect to the strong and weak axes and k_{yy}, k_{zz}, k_{yz}, k_{zy} are the interaction factors accounting for the slenderness of the member and shape of the bending moment diagram, as reported in table B.1 of Annex B in Eurocode 3.

The lateral torsional stability (TI) index is calculated as

$$TI = max\begin{cases} \dfrac{N_{Ed}(t)}{N_{b,Rd,y}} + k_{yy}\dfrac{M_{Ed,y}(t)}{\chi_{LT}M_{pl,Rd,y}} + k_{yz}\dfrac{M_{Ed,z}(t)}{M_{pl,Rd,z}} \\ \dfrac{N_{Ed}(t)}{N_{b,Rd,z}} + k_{zy}\dfrac{M_{Ed,y}(t)}{\chi_{LT}M_{pl,Rd,y}} + k_{zz}\dfrac{M_{Ed,z}(t)}{M_{pl,Rd,z}} \end{cases} \tag{30}$$

where χ_{LT} is the reduction factor due to lateral torsional buckling, as reported in Eurocode 3 (6.3.2). The interaction factors k_{yy}, k_{zz}, k_{yz}, k_{zy} are determined as reported in table B.2 of Annex B in Eurocode 3 for members susceptible to lateral torsional buckling.

7. Effects of uncertainties

To estimate the effects of the uncertainties, results of analyses type #1 and #2 are compared. The comparison is separately carried out in terms of global and local response parameters. Three limit states are considered to assess the seismic performance of the building, i.e. (1) damage limitation (DL), significant damage (SD) and near collapse (NC) limit states.

7.1. Global response parameters

The fragility curves corresponding to the achievement of a maximum interstorey drift angle δ equal to 0.5%, 2.5% and 5.0% and to a residual interstorey drift angle δ_r equal to 0.5% are plotted in Fig. 4. The first value of the maximum interstorey drift angle (0.5%) is consistent with the limit value adopted in the phase of design and is considered as representative of the DL limit state.

In the absence of specifications in Eurocode 8 on interstorey drifts corresponding to the achievement of SD and NC limit states, the other two values of the limit interstorey drift (2.5 and 5.0%) are based on recommendations of FEMA 356 for the Life Safety and Collapse Prevention Limit states of steel MRFs. A residual interstorey drift angle δ_r equal to 0.5% is assumed as corresponding to the achievement of the SD limit state.

The seismic intensity measure considered in the figure is the pseudo-acceleration corresponding to the first period of vibration of the numerical model used in analysis type #1. This period of vibration is equal to 1.414 s and 2.132 s in the 3-storey and 5-storey buildings, respectively. The period of vibration of the systems considered in analysis type #2 ranges from 1.313 s to 1.485 s (median value equal to 1.413 s and COV = 0.027) in the 3-storey building and from 2.046 s to 2.228 s (median value equal to 2.138 s and COV = 0.019) in the 5-storey building.

The comparison between the fragility curves obtained by the model with median properties of the uncertain variables (black line in the figures) and the fragility curves obtained by models with uncertain values of the same variables (red dashed lines) shows that the uncertainties have a minor effect on the fragility curves in terms of global response parameters. Specifically, the ratios of the values of the parameters θ and β derived by analysis type #1 (θ_M and β_{RTR}) to the corresponding values (θ_{unc} and β_{unc}) derived by analysis type #2 (Fig. 5) are on average equal to 1.00 and 0.98, respectively. As a consequence, no significant error is committed in the estimate of the mean annual frequency of exceedance (see Table 2) if the uncertainties of the seismic mass, permanent and variable loads, equivalent viscous damping ratio and strength of steel are neglected. It is interesting to underline that this result confirms the finding obtained in [21] with reference to MRFs designed according to the ASCE code and in which only the variability of the cyclic response of the plastic hinges was considered. In any case, the mean annual frequency of exceedance of the considered limit states is smaller than the target value provided in CNR-DT-2012 [32].

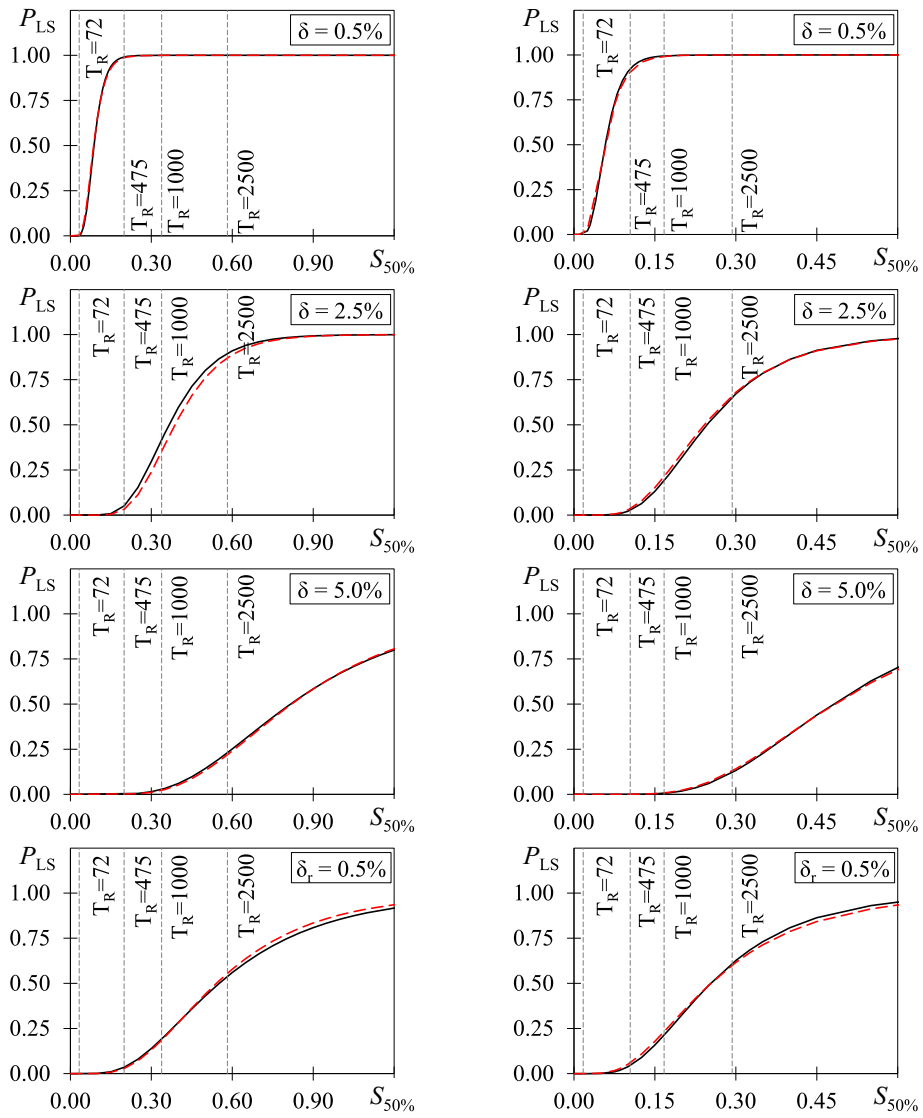

Fig. 4. Fragility curves corresponding to the achievement of the considered limit values in the global response parameters (transient interstorey drift angle δ and residual interstorey drift angle δ_r).
Notes: (solid black line) model with median properties of the uncertain variables (dashed red line) model with random values of the uncertain variables.

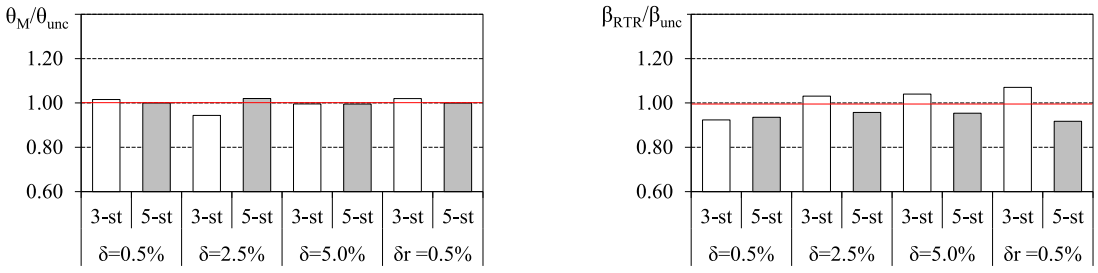

Fig. 5. Influence of the uncertain variables on the parameter θ and β of the fragility curves for global response parameters (transient interstorey drift angle δ).

7.2. Local response parameters

The achievement of the SD limit state is associated with the achievement of either significant damage of ductile members (DI = 0.75 or PI = 0.75) or instability of columns (SI = 1.00 or TI = 1.00). The NC limit state is associated with either failure of dissipative members (DI = 1.00 or PI = 1.00) or instability of columns (SI = 1.00 or TI = 1.00).

The fragility curves corresponding to the achievement of a maximum damage index DI equal to either 0.75 or 1.00 at the ends of beams and columns and to the achievement of a stability index equal to 1.00 in columns are plotted in Fig. 6. No fragility curve is plotted in terms of the damage index of the panel zone because yielding of the panel zone has never occurred during the numerical analysis.

Independently of the considered model, for each considered intensity measure of the seismic event the number of ground motions leading to the lateral torsional buckling of the columns of the first storey is always

Table 2
Mean annual frequency of exceedance of the considered limit states referred to global response parameters: comparison between model M with median values of the additional uncertain variables and model U with random values of the uncertain variables.

	$\lambda_{0.5\%} \times 10^{-3}$		$\lambda_{2.5\%} \times 10^{-3}$		$\lambda_{r=0.5\%} \times 10^{-3}$		$\lambda_{5.0\%} \times 10^{-3}$	
Target	45.0		4.7		4.7		2.3	
Model	3-st.	5-st.	3-st.	5-st.	3-st.	5-st.	3-st.	5-st.
M	5.75	4.88	1.00	0.82	0.66	0.84	0.34	0.30
U	5.90	4.94	0.92	0.86	0.66	0.88	0.33	0.31
Error	−2.63%	−1.20%	9.06%	−4.22%	0.78%	−4.13%	2.39%	−1.14%

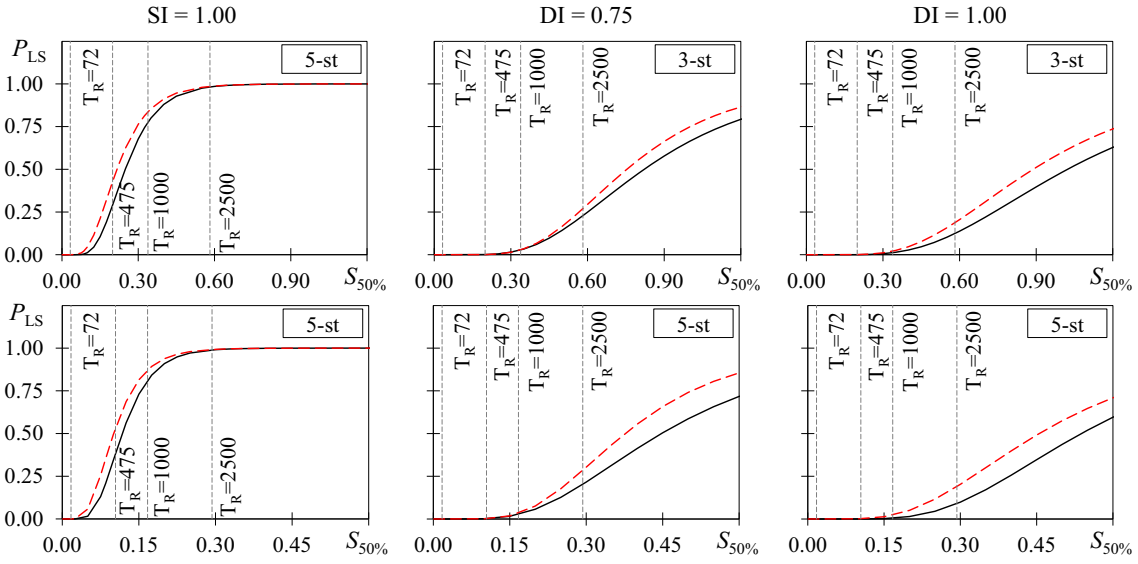

Fig. 6. Fragility curves corresponding to the achievement of the considered limit values in the local response parameters (stability index SI and damage index DI). Notes: (solid black line) model with median properties of the uncertain variables (dashed red line) model with random values of the uncertain variables.

larger than the number of the ground motions leading to the full exploitation of the plastic rotation capacity of beams and columns. This result supports the proposal of some other researchers [40] who suggest the use of a reduced cross-section at the base of the first storey column to improve the seismic performance of MRFs.

The median pseudo-acceleration leading to a stability index equal to 1.0 is larger than that corresponding to seismic events with $T_R = 475$ years, whereas it is smaller than that corresponding to seismic events with $T_R = 1000$ years (i.e. probability of occurrence of 5% in 50 years). In the Italian Seismic code, this latter value of T_R is associated with the NC limit state. The comparison between the fragility curves obtained by the model with median properties of the uncertain variables (black line in the figure) and the fragility curves obtained by the models with uncertain values of the same variables (red dashed line in the figure) shows that the uncertainty mainly affects the median value of the pseudo-acceleration leading to the considered limit state, whereas it has a minor effect on the parameter β. Indeed, the ratios θ_M / θ_{unc} and $\beta_{RTR} / \beta_{unc}$ are on average equal to 1.16 and 1.00, respectively (Fig. 7). The overestimation of the median pseudo-acceleration corresponding to the considered limit states leads to an underestimation of the mean annual frequency of exceedance up to 26%, as reported in Table 3. Further, in the case of the 5-storey model the mean annual frequency of exceedance of the limit condition characterised by SI = 1.00 is higher than the target

Table 3
Mean annual frequency of exceedance of the considered limit states referred to local response parameters: comparison between model M with median values of the additional uncertain variables and model U with random values of the uncertain variables.

	$\lambda_{SI=1.00} \times 10^{-3}$		$\lambda_{DI=0.75} \times 10^{-3}$		$\lambda_{DI=1.00} \times 10^{-3}$	
Target	2.3		4.7		2.3	
Model	3-storey	5-storey	3-storey	5-storey	3-storey	5-storey
M	1.713	2.120	0.334	0.368	0.243	0.262
U	2.110	2.629	0.367	0.446	0.300	0.356
Error	−18.8%	−19.4%	−9.0%	−17.6%	−19.0%	−26.4%

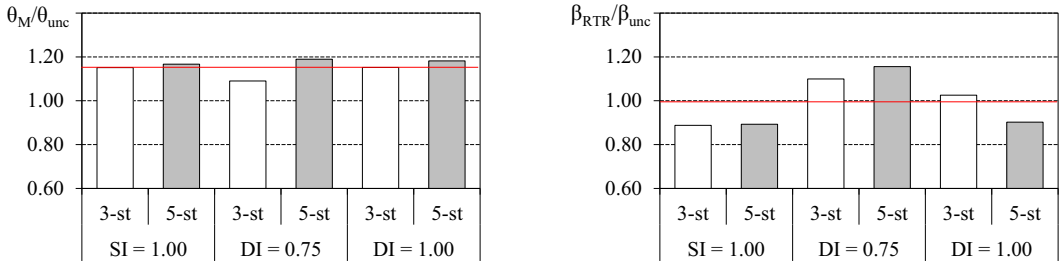

Fig. 7. Influence of the uncertain variables on the parameter θ and β of the fragility curves for local response parameters (stability index SI and damage index DI).

value if the uncertain variables are considered, whereas it is lower than the target value if the model with median values of the variables is used.

8. Estimate of the dispersion related to the single variable

Results of analysis type #3 quantify the dispersion of the results because of the uncertainties in the material strength (β_{mat}), equivalent viscous damping ratio (β_ξ) and loads (β_L), separately considered. The values obtained are plotted in Fig. 8 where, for the sake of comparison, the dispersion due to the record-to-record uncertainty is also reported.

The figure shows that, apart from the record-to-record uncertainty, the uncertainty that mainly affects the dispersion of the results is the equivalent viscous damping ratio. In the worst case, the value of β_ξ is close to 0.20. The uncertainty in the material properties has a negligible effect on the parameter β of the fragility curves referring to a prefixed value of the interstorey drift angle (β_{mat} lower than 0.05) and has a maximum effect on the parameter β of the fragility curves referring to local parameters. When considering the uncertainty in the loads, values of β_L are up to 0.1 and are obtained in the fragility curves referring to global response parameters. In any case, these dispersions are much smaller than those due to record-to-record variability.

The above dispersions are used to estimate the total uncertainty

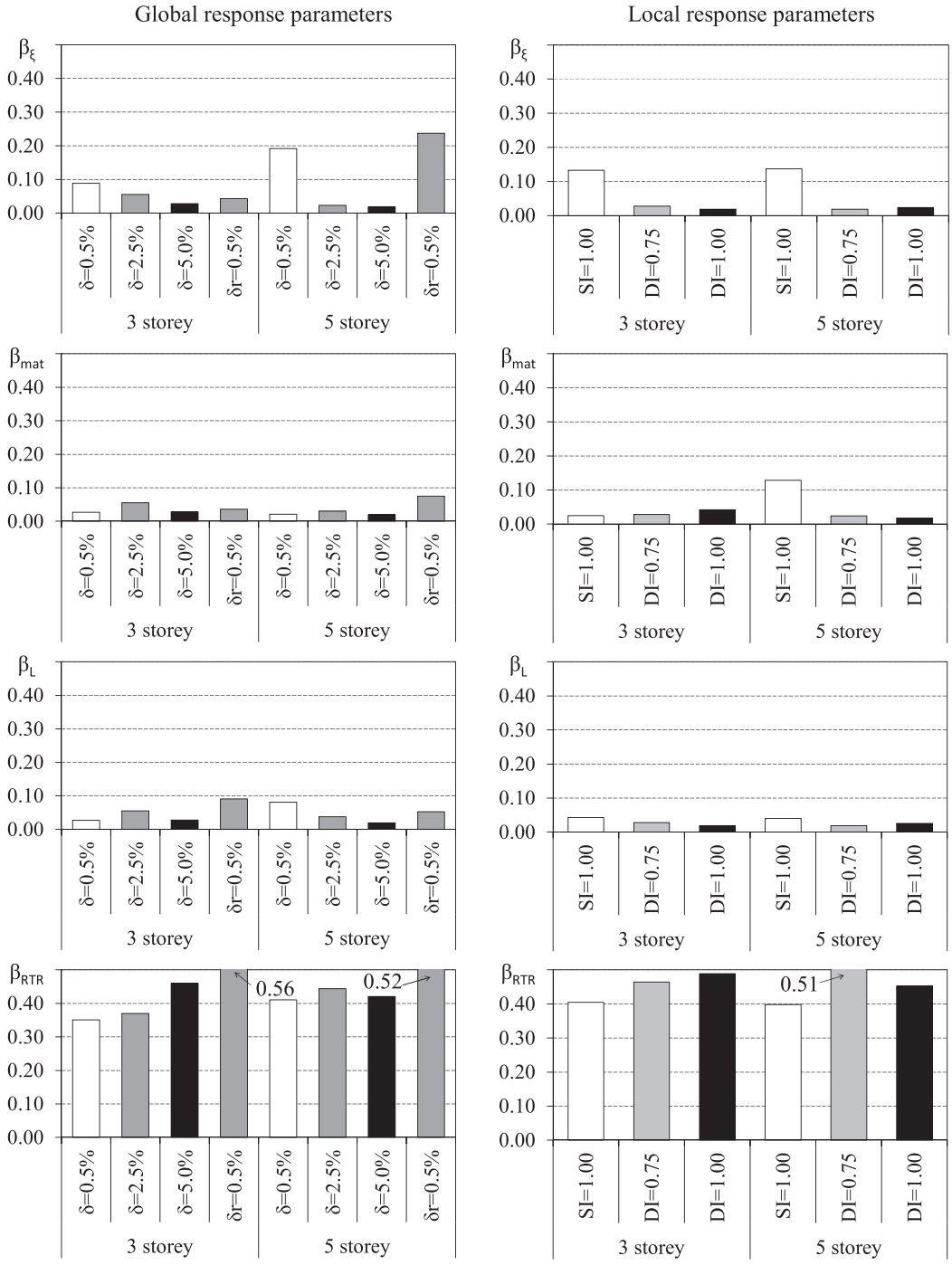

Fig. 8. Dispersion of the intensity measure caused by the single source of uncertainty.

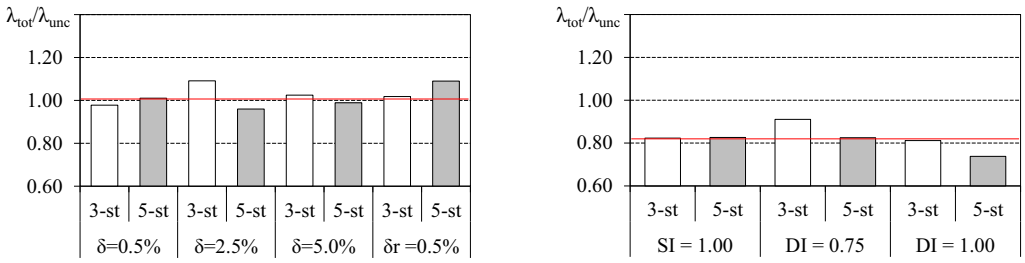

Fig. 9. Mean annual frequency of exceedance of the considered limit states by means of the simplified approach reported in FEMA documents.

$$\beta_{tot} = \sqrt{\beta_{RTR}^2 + \beta_{mat}^2 + \beta_{\xi}^2 + \beta_L^2} \quad (31)$$

Finally, the mean annual frequency of exceedance of the considered limit states has been determined based on the fragility curves characterised by median pseudo-acceleration θ_M and total dispersion β_{tot}. The obtained values (λ_{tot}) are compared in Fig. 9 with the ones corresponding to the fragility curves resulting from analysis type #2, i.e. where the uncertain variables are explicitly taken into account. The figure shows that, if the simplified approach is used, the mean annual frequency of exceedance of the global response parameters are slightly overestimated (average $\lambda_{tot}/\lambda_{unc}$ equal to 1.02), whereas the mean annual frequency of exceedance of the local response parameters are underestimated (average $\lambda_{tot}/\lambda_{unc}$ equal to 0.82).

9. Proposal of a simplified approach

Referring to simplified approaches that intend to mime the results of a full probabilistic analyses by means of modifications of parameters θ and β of fragility curves resulting from record-to-record variability only, some proposals are formulated herein by the authors.

In particular, based on the results of analyses type #1 and #2, the authors suggest dividing the median value of the intensity measure (θ) leading to the achievement of the considered limit state (because of only record-to-record uncertainty) by a factor equal to 1.2, whereas no modification is suggested for the dispersion β. Such modifications are required if local response parameters are assessed, whereas no modification is needed if global response parameters are considered. To prove the validity of the proposal, the mean annual frequencies of exceedance of the SD and NC limit states in the systems under investigation are recalculated here and reported in Table 4. The analysis of the data in the table shows that the proposal leads to a satisfactory prediction of the mean annual frequency of exceedance of the examined limit states.

10. Conclusions

The present paper investigates the probabilistic assessment of the seismic performance of steel MRFs designed according to Eurocodes. The considered MRFs are three- and five-storey high and are analysed by the multiple stripe method of analysis by means of sets of earthquake ground motions that depend, in the main properties, on the value of the seismic intensity measure. Additional uncertainties are considered for the mechanical properties of steel, dead loads, live loads and equivalent viscous damping ratio. Criteria are defined to assess the performance at the achievement of different limit states in terms of interstorey drifts and damage indexes. To reach a synthetic evaluation of the seismic performances the mean annual frequency of exceedance of the assigned limit state condition is also evaluated.

The main conclusions of the numerical analyses are:

- the comparison between the fragility curves obtained by the model with median properties of the additional uncertain variables (i.e. mechanical properties of steel, dead loads, live loads and equivalent viscous damping ratio) and the fragility curves obtained by models with uncertain values of the same variables shows that the additional uncertainties have a minor effect on the fragility curves in terms of global response parameters.
- the comparison between the fragility curves obtained by the model with median properties of the additional uncertain variables and the fragility curves obtained by the models with uncertain values of the same variables shows that the uncertainty mainly affects the median value of the fragility curves in terms of local response parameters. The uncertainties have a minor effect on the parameter β of the fragility curves. This result supports the belief that the assumption that the median-parameter model produces the median seismic performance is not true if local response parameters are investigated.
- apart from the record-to-record uncertainty, the uncertainty in the equivalent viscous damping ratio appears to affects the dispersion of the results more significantly than the uncertainty in the other additional uncertain variables.
- if the total dispersion in the results is estimated as the SRSS of the dispersions caused by the single uncertain variables, the mean annual frequency of exceedance of the global response parameters is slightly overestimated, whereas the mean annual frequencies of exceedance of the local response parameters is underestimated.
- if the seismic performance is assessed based on the only record-to-record variability, the median value of the intensity measure leading to the achievement of limit values of local response parameters should be divided by a factor equal to 1.2 to mime the results of a full probabilistic analyses. No modification is needed for the median value of the intensity measure and dispersion of fragility curves referring to global response parameters.

Table 4
Mean annual frequency of exceedance of the considered limit states referred to local response parameters: comparison between proposed approach and model U with random values of the uncertain variables.

	$\lambda_{SI=1.00} \times 10^{-3}$		$\lambda_{DI=0.75} \times 10^{-3}$		$\lambda_{DI=1.00} \times 10^{-3}$	
Target	2.3		4.7		2.3	
	3-st.	5-st.	3-st.	5-st.	3-st.	5-st.
Proposed model	2.157	2.651	0.429	0.482	0.323	0.347
Error	2.22%	0.84%	17.2%	7.95%	7.94%	−2.49%

Credit author statement

The authors equally contributed to the research paper.

Declaration of Competing Interest

The authors declare that they have no known competing financial interests or personal relationships that could have appeared to influence the work reported in this paper.

Data availability

Data will be made available on request.

References

[1] S.S.F. Mehanny, A.S. Ayoub, Variability in inelastic displacement demands: uncertainty in system parameters versus randomness in ground records, Eng. Struct. 30 (2008) 1002–1013.

[2] B. Asgarian, B. Ordoubadi, Effects of structural uncertainties on seismic performance of steel moment resisting frames, J. Constr. Steel Res. 120 (2016) 132–142.

[3] S. Dastmalchi, H.V. Burton, Effect of modeling uncertainty on multi-limit state performance of controlled rocking steel braced frames, J. Build. Eng. 39 (2021), 102308.

[4] E.I. Katsanos, A.G. Sextos, G.D. Manolis, Selection of earthquake ground motion records: a state-of-the-art review from a structural engineering perspective, Soil Dyn. Earthq. Eng. 30 (4) (2010) 157–169.

[5] B. Ellingwood, T.V. Galambos, J.G. MacGregor, C.A. Cornell, Development of a Probability-Based Load Criterion for American National Standard A58, National Bureau of Standards, Washington, DC, 1980.

[6] CEN, EN 1990:2002+A1. Eurocode - Basis of Structural Design, European Committee for Standardization, Bruxelles, 2005.

[7] M. Badalassi, A. Braconi, L.G. Cajot, S. Caprili, H. Degee, M. Gundel, M. Hjiaj, B. Hoffmeister, S.A. Karamanos, W. Salvatore, H. Somja, Influence of variability of material mechanical properties on seismic performance of steel and steel–concrete composite structures, Bull. Earthq. Eng. 15 (2017) 1559–1607.

[8] L. Simões da Silva, C. Rebelo, D. Nethercot, L. Marques, R. Simões, P.M.M. Vila Real, Statistical evaluation of the lateral–torsional buckling resistance of steel I-beams, part 2: variability of steel properties, J. Constr. Steel Res. 65 (2009) 832–840.

[9] M.P. Byfield, Steel Design and Reliability Using Eurocode 3, Ph.D. thesis., University of Nottingham, 1996.

[10] F.M. Mazzolani, E. Mele, V. Piluso, Statistical characterization of constructional steels for structural ductility control, Costruzioni Metalliche 2 (1983) 89–101.

[11] J. Melcher, Z. Kala, M. Holicky, M. Fajkus, L. Rozlivka, Design characteristics of structural steels based on statistical analysis of metallurgical products, J. Constr. Steel Res. 60 (2004) 795–808.

[12] D.G. Lignos, H. Krawinkler, Sidesway collapse of deteriorating structural systems under seismic excitations, in: Rep. No. TB 177, The John A. Blume Earthquake Engineering Center, Stanford University, Standford CA, 2012.

[13] K.A. Porter, J.L. Beck, R.V. Shaikhutdinov, Sensitivity of building loss estimates to major uncertain variables, Earthquake Spectra 18 (4) (2002) 719–743.

[14] G.H. McVerry, Frequency Domain Identification of Structural Models for Earthquake Records, Report No. EERL 79-02, California Institute of Technology, Pasadena, CA, 1979. http://caltecheerl.library.caltech.edu/documents/disk0/00/00/02/23/00000223-00/7902.pdf.

[15] R.E. Melchers, Structural Reliability Analysis and Prediction (Second Edition), John Wiley & Sons, 2002. ISBN: 0 471 98771 9.

[16] L. Faravelli, Response surface approach for reliability analysis, J. Eng. Mech. (ASCE) 115 (1989) 2763–2781.

[17] S. De Grandis, M. Domaneschi, F. Perotti, A numerical procedure for computing the fragility of NPP components under random seismic excitation, Nucl. Eng. Des. 239 (2009) 2491–2499.

[18] F. Perotti, M. Domaneschi, S. De Grandis, The numerical computation of seismic fragility of base-isolated. Nuclear power plants buildings, Nucl. Eng. Des. 262 (2013) 189–200.

[19] FEMA P-58-1, Seismic Performance Assessment of Buildings, Volume 1 – Methodology, Federal Emergency Management Agency, Washington, DC, 2022.

[20] FEMA P695, Quantification of Building Seismic Performance Factors, Federal Emergency Management Agency, Washington, D.C, 2022.

[21] A.K. Kazantzi, D. Vamvatsikos, D.G. Lignos, Seismic performance of a steel moment-resisting frame subject to strength and ductility uncertainty, Eng. Struct. 78 (2014) 69–77.

[22] M.S. Pandikkadavath, K.M. Shaijal, S. Mangalathu, R. Davis, Seismic robustness assessment of steel moment resisting frames employing material uncertainty incorporated incremental dynamic analysis, J. Constr. Steel Res. 191 (2022), 107200.

[23] S.R.H. Vaez, A.A. Samani, S.A. Mobinipour, E. Dehghani, Effect of uncertainties in design variables on the hysteresis response of 2D steel moment-resisting frames, Pract. Period. Struct. Design Constr. ASCE 27 (4) (2022) 04022044.

[24] FEMA 450, NEHRP Recommended Provisions for Seismic Regulations for New Buildings and Other Structures, Building Seismic Safety Council, Washington, DC, 2003.

[25] A. Skiadopoulos, A. Elkady, D.G. Lignos, Proposed panel zone model for seismic design of steel moment-resisting frames, J. Struct. Eng. 147 (4) (2021) 04021006.

[26] J.W. Baker, Efficient analytical fragility functions fitting using dynamic structural analysis, Earthquake Spectra 31 (1) (2015) 579–599.

[27] D. Straub, A. Der Kiureghian, Improved seismic fragility modeling from empirical data, Struct. Saf. 30 (4) (2008) 320–336.

[28] CEN, EN 1998-1. EuroCode 8: Design of Structures for Earthquake Resistance – Part 1: General Rules, Seismic Actions and Rules for Buildings, European Committee for Standardization, Bruxelles, 2004.

[29] C. Meletti, V. Montaldo, Stime di pericolosità sismica per diverse probabilità di superamento in 50 anni: valori di ag. Progetto DPC-INGV S1, Deliverable D2. http://esse1.mi.ingv.it/d2.html, 2007.

[30] D. Spallarossa, S Barani, 2007. Disaggregazione della pericolosità sismica in termini di M-R-ε. Progetto DPC-INGV S1, Deliverable D14. http://esse1.mi.ingv.it/d14.html.

[31] F. Barbagallo, M. Bosco, E.M. Marino, P.P. Rossi, Variable vs. invariable elastic response spectrum shapes: impact on the mean annual frequency of exceedance of limit states, Eng. Struct. 214 (2020), 110620.

[32] CNR-DT 212/2013, Istruzioni per la Valutazione Affidabilistica di Edifici Esistenti, Consiglio Nazionale delle Ricerche, Roma, 14 maggio, 2014.

[33] D. Gasparini, E.H. Vanmarcke, SIMQKE: A Program for Artificial Motion Generation. Users's Manual and Documentation, Department of Civil Engineering, 1976.

[34] D.M. 17/01/2018, Norme Tecniche per le costruzioni (Provisions for constructions). Rome, 2018 (in Italian).

[35] S. Mazzoni, F. McKenna, M.H. Scott, G.L. Fenves, et al., OpenSees Command Language Manual, Pacific Earthquake Engineering Research Center, University of California, Berkeley, 2007.

[36] F. Barbagallo, M. Bosco, E.M. Marino, P.P. Rossi, On the fibre modelling of beams in RC framed buildings with rigid diaphragm, Bull. Earthq. Eng. 18 (1) (2020) 189–210.

[37] A. Gupta, E. Krawinkler, Report n. 132. Stanford Engineering, Blume Earthquake Engineering Center, 1999.

[38] prEN1998-1-2 SC8 24-02-2021, Eurocode 8: Earthquake Resistance Design of Structures, CEN/TC 250/SC 8, 2022.

[39] CEN, ENV 1993-1-1. EuroCode 3: Design of Steel Structures - Part 1–1: General Rules and Rules for Buildings, European Committee for Standardization, Bruxelles, 2005.

[40] M. D'Aniello, R. Tartaglia, R. Landolfo, L. Di Sarno, A. Le Maoult, G. Rastiello, Preliminary results from shake table tests of the FUTURE mock-up, in: Proceedings of the 10th International Conference on Behaviour of Steel Structures in Seismic Areas, 2022.